

ATMOSPHERIC LOSS OF EXOPLANETS RESULTING FROM STELLAR X-RAY AND EXTREME-ULTRAVIOLET HEATING

H. LAMMER,¹ F. SELSIS,² I. RIBAS,³ E. F. GUINAN,⁴ S. J. BAUER,⁵ AND W. W. WEISS⁶

Received 2003 July 11; accepted 2003 October 17; published 2003 November 13

ABSTRACT

Past studies addressing the thermal atmospheric escape of hydrogen from “hot Jupiters” have been based on the planet’s effective temperature, which, as we show here, is not physically relevant for loss processes. In consequence, these studies led to significant underestimations of the atmospheric escape rate ($\leq 10^3 \text{ g s}^{-1}$) and to the conclusion of long-term atmospheric stability. From more realistic exospheric temperatures, determined from X-ray and extreme-ultraviolet (XUV) irradiation and thermal conduction in the thermosphere, we find that energy-limited escape and atmospheric expansion arise, leading to much higher estimations for the loss rates ($\approx 10^{12} \text{ g s}^{-1}$). These fluxes are in good agreement with recent determinations for HD 209458b based on observations of its extended exosphere. We also show that for young solar-type stars, which emit stronger XUV fluxes, the inferred loss rates are significantly higher. Thus, hydrogen-rich giant exoplanets under such strong XUV irradiances may evaporate down to their core sizes or shrink to levels at which heavier atmospheric constituents may prevent hydrodynamic escape. These results could explain the apparent paucity of exoplanets so far detected at orbital distances less than 0.04 AU.

Subject headings: astrobiology — conduction — hydrodynamics — instabilities — planetary systems

1. INTRODUCTION

The recent observation of an extended and hydrogen-evaporating atmosphere for HD 209458b raises the question of atmospheric stability against escape at very short orbital distances (Guillot et al. 1996; Wuchterl, Guillot, & Lissauer 2000; Hubbard, Burrows, & Lunine 2002; Del Popolo & Eksi 2002; Vidal-Madjar et al. 2003). In former studies of close-in exoplanets, the radiative effective temperature (T_{eff}) was used to estimate the atmospheric evaporation rates. However, it is the exosphere temperature (T_{∞}), usually much higher than T_{eff} , that is responsible for thermal escape processes, also suggested by Schneider et al. (1998) and Moutou et al. (2001). For example, Jupiter’s observed $T_{\infty} \approx 700\text{--}1000 \text{ K}$ (Smith & Hunten 1990) is actually close to the expected value of T_{eff} for 51 Peg b. For terrestrial planets, T_{∞} depends solely on the X-ray and extreme-ultraviolet (XUV) flux, but additional heating sources, mostly related to accelerated particles and atmospheric gravity waves, become important for giant planets in the outer solar system (Atreya, Pollack, & Matthews 1989; Johnson 1990). Because the efficiencies of such additional heating sources are different for each planet, we consider here only the external energy source.

To estimate the XUV contribution to the exospheric heating, we use a scaling law based on an approximate solution of the heat balance equation in planetary upper atmospheres (Bauer 1971; Gross 1972). This method has been shown to apply to solar system planets (Gross 1972, 1974; Bauer 1973; Bauer & Hantsch 1989) and is applied for the first time to estimate the values of $T_{\text{XUV}\infty}$ for exoplanets. This estimation of $T_{\text{XUV}\infty}$ is used

to check for the onset of atmospheric blow-off conditions (e.g., Öpik 1963; Chamberlain 1963; Watson, Donahue, & Walker 1981; Zahnle, Kasting, & Pollack 1990) in hydrogen-rich close-in giant exoplanets. When this is the case, we adopt a hydrodynamic model for the calculation of the temperature and atmospheric escape, as the scaling law discussed above is no longer applicable.

2. XUV HEATING OF UPPER PLANETARY ATMOSPHERES

The effective heat production below the exosphere is balanced by the divergence of the conductive heat flux of the XUV radiation, which leads to the following expression for $T_{\text{XUV}\infty}$ (Gross 1972, 1974):

$$T_{\text{XUV}\infty}^s = \frac{s\epsilon\alpha k}{K_0 m_i g} \int_{\lambda_1}^{\lambda_2} d\lambda I_{\text{XUV}}(\lambda) \left\{ E[\tau(\lambda)] + \ln[\tau(\lambda)] + \gamma - \frac{m_i}{m_j} [1 - e^{-\tau(\lambda)}] \right\} + T_0^s, \quad (1)$$

where λ is the wavelength, τ is the optical thickness, E is the exponential integral, γ is Euler’s constant, ϵ is the heating efficiency, k is the Boltzmann constant, and m_i and m_j are the masses of the atmospheric constituents. Also in equation (1), $K(T) = K_0 T^s$ is the thermal conductivity coefficient, s depends on the thermospheric composition, g is the gravitational acceleration, I_{XUV} is the XUV intensity at the orbital distance considered, and T_0 is the temperature at the base of the thermosphere. In the case of a hydrogen-dominated thermosphere $i \approx j$ (Gross 1972).

The factor α takes on values appropriate for the rotation of the planet: about $\frac{1}{4}$ for rapidly rotating planets such as Jupiter (Gross 1972; Bauer 1973) and about $\frac{1}{2}$ for slowly rotating or tidally locked planets (because of the ratio to the cross section area of the surface of the planetary sphere; Bauer 1973). The value of α may be reduced close to $\frac{1}{4}$ by the action of strong thermospheric winds expected at close orbital distances (e.g., Cho et al. 2003).

¹ Space Research Institute, Austrian Academy of Sciences, Schmiedlstrasse 6, A-8042 Graz, Austria; helmut.lammer@oeaw.ac.at.

² Centro de Astrobiología (INTA-CSIC), Carretera de Ajalvir, km 4, 28850 Torrejón de Ardoz, Madrid, Spain; selsis@obs.u-bordeaux1.fr.

³ Departament d’Astronomia i Meteorologia, Universitat de Barcelona, Av. Diagonal 647, 08028 Barcelona, Spain; iribas@am.ub.es.

⁴ Department of Astronomy and Astrophysics, Villanova University, 800 Lancaster Avenue, Villanova, PA 19085; edward.guinan@villanova.edu.

⁵ Institute for Geophysics, Astrophysics and Meteorology, University of Graz, Universitätsplatz 5, A-8010 Graz, Austria; siegfried.bauer@uni-graz.at.

⁶ Department for Astronomy, University of Vienna, Türkenschanzstrasse 17, A-1180 Vienna, Austria; weiss@astro.univie.ac.at.

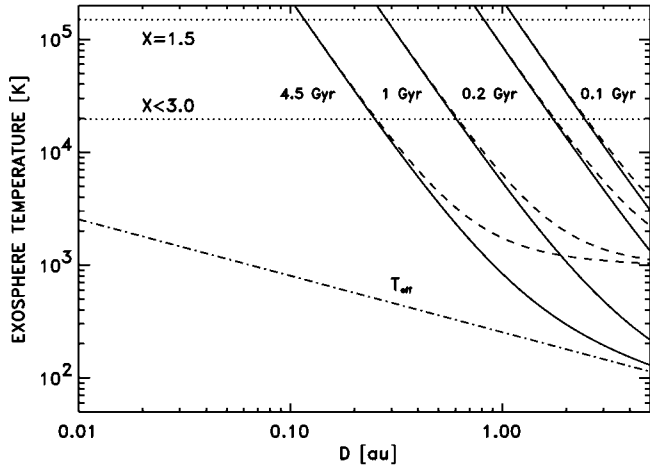


FIG. 1.—Scaled $T_{\text{XUV},\infty}$ and T_{∞} for Jupiter-class exoplanets are shown as a function of orbital distance for Sunlike stars with ages of 4.5, 1, 0.2, and 0.1 Gyr. The corresponding XUV fluxes are 1, 6, 50, and 100 times the present value. *Dashed lines*: T_{∞} calculated by scaling solely the XUV contribution and assuming the additional heating sources to be a constant term. *Solid lines*: Only the scaled $T_{\text{XUV},\infty}$. As can be seen, regardless of the case considered, the exosphere temperature reaches blow-off conditions (*dotted lines*). *Dashed-dotted line*: T_{eff} , which is much smaller than T_{∞} at close orbital distances.

After some approximations, one obtains (Bauer 1971, 1973; Bauer & Hantsch 1989)

$$T_{\text{XUV},\infty}^s \approx \frac{\varepsilon \alpha I_{\text{XUV}} k \sigma_c}{K_0 m_i g \sigma_a} + T_0^s, \quad (2)$$

in which σ_c and σ_a are the collision and absorption cross sections, respectively, and I_{XUV} is the XUV intensity at the planet's orbital distance.

As a check, we investigated possible cooling arising from the production and decay of H_3^+ ions, which are observed in the auroral regions of giant planets (Stallard et al. 2002). In the case of “hot Jupiters,” however, thermal dissociation of H_2 strongly limits the production of H_3^+ (involving H_2 and H_2^+ produced by energetic electrons). It is therefore unlikely that a significant fraction of the large amount of energy deposited from the XUV (including $\text{H I Ly}\alpha$ 121.6 nm) can be reemitted in the IR bands of H_3^+ .

Bauer (1971) and Bauer & Hantsch (1989) showed that when planets 1 and 2 have thermospheres with comparable gas compositions, the following scaling relation is applicable:

$$\frac{(T_{\text{XUV},\infty}^s - T_0^s)_1}{(T_{\text{XUV},\infty}^s - T_0^s)_2} \approx \frac{I_{\text{XUV}1} g_2}{I_{\text{XUV}2} g_1}. \quad (3)$$

Equations (1)–(3) indicate that $T_{\text{XUV},\infty}$ depends on I_{XUV} , which decreases with the distance from the star, and on g , which is related to the mass and radius of the planet.

3. EVOLUTION OF THE STELLAR XUV FLUX

The time dependence of I_{XUV} is critical to the evolution of thermal escape during the history of a planetary system (Lammer et al. 2003a). Estimates of the solar high-energy flux evolution (Simon, Boesgaard, & Herbig 1985) are indirectly possible by the study of stellar proxies for the Sun at different ages. Multiwavelength (from X-rays to the UV) observations have been collected for a sample of solar proxies within the

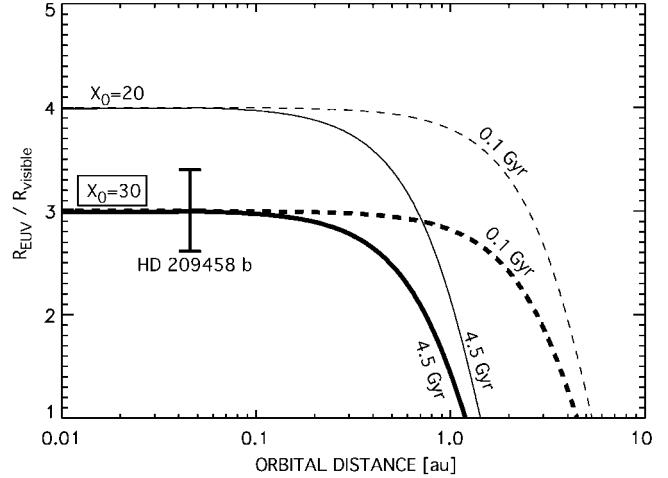


FIG. 2.—XUV-driven expansion of the upper atmosphere illustrated for a hot Jupiter with the mass of HD 209458b. The curves show the ratio, given by the hydrodynamic expansion model, between the altitude R_{EUV} (where most of the XUV is absorbed) and the altitude R_{vis} , where the visible opacity is 1. The computed expansion depends on the XUV flux (and thus on the age of the star) and also on X_0 (see text), which is a dimensionless parameter of the model constrained in the range 20–30. The solid and dashed lines correspond to a 4.5 and 0.1 Gyr solar-type star, respectively. The thick and thin lines show the atmospheric expansion for $X_0 = 30$ and 20, respectively.

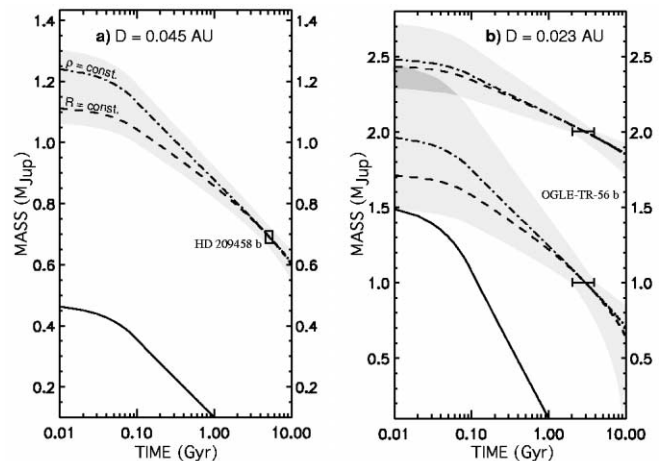


FIG. 3.—Long-term evolution of the mass of hot Jupiters from XUV-driven thermal escape. For a given set of parameters characterizing an exoplanet at a given age τ (r_{pi} : radius, M : mass, D : orbital distance), one can calculate the mass evolution by assuming (1) that the only loss process is energy-limited escape, (2) a mass-radius relation, (3) a constant orbital distance, and (4) a hydrogen-rich atmosphere. The observed parameters for HD 209458b (a) are $r_{\text{pi}} = 1.43 \pm 0.04 R_{\text{Jup}}$, $M = 0.69 \pm 0.02 M_{\text{Jup}}$, and $\tau = 5.2$ Gyr (Cody & Sasselov 2002). For OGLE-TR-56b (b), we adopted $r_{\text{pi}} = 1.3 \pm 0.15 R_{\text{Jup}}$, $M = 0.9 \pm 0.3 M_{\text{Jup}}$, and $\tau = 3 \pm 1$ Gyr (Konacki et al. 2003; Sasselov 2003). The dashed and dash-dotted lines show the evolution obtained with the mean observed parameters, considering, respectively, a constant radius or density. *Shaded area*: Envelope of all possible evolution scenarios within the uncertainties of the planetary parameters. *Solid curve*: Evolution of a gaseous planet at the same orbital distance with a constant density of 0.3 g cm^{-3} , which fully evaporates after 1 Gyr. In the case of OGLE-TR-56b, whose nature is still in debate, our calculations yield an initial mass of $2.5 \pm 0.2 M_{\text{Jup}}$ if its current mass turned out to be twice the value determined by Konacki et al. (2003).

Sun in Time program (Guinan & Ribas 2002) containing stars that represent most of the Sun's main-sequence lifetime from ~ 130 Myr to 8 Gyr. The resulting relative XUV fluxes yield an excellent correlation between the emitted flux and stellar age. In the 1–1000 Å interval, the fluxes follow a power-law relationship of the form

$$\frac{I_0(t)}{I_0} = 6.16[t(\text{Gyr})]^{-1.19}. \quad (4)$$

At longer wavelengths, the H I Ly α emission feature can contribute a significant fraction of the XUV flux. For a few of the *Sun in Time* targets, high-resolution *Hubble Space Telescope* spectroscopic observations were used to estimate the net stellar flux. These measurements, together with the observed solar Ly α integrated flux, accurately define a power-law relationship

$$\frac{I_{L_\alpha}(t)}{I_{L_\alpha}} = 3.17[t(\text{Gyr})]^{-0.75}. \quad (5)$$

In both of these XUV and Ly α flux-age relations, which are valid for solar-type stars with ages between 0.1 and 8 Gyr, I_0 and I_{L_α} are the present solar integrated fluxes at 1 AU and $I_0(t)$ and $I_{L_\alpha}(t)$ are the integrated fluxes as a function of time. For our study, we consider $I_{\text{XUV}}(t) = I_0(t) + I_{L_\alpha}(t)$. The above relationships are in good agreement with previous studies (Zahnle & Walker 1982; Ayres 1997) and indicate fluxes of $\approx 6I_0$ and $\approx 3I_{L_\alpha}$ about 3.5 Gyr ago, and $\approx 100I_0$ and $\approx 20I_{L_\alpha}$ about 100 Myr after the Sun's arrival on the main sequence.

4. ESTIMATION OF THE XUV FLUX CONTRIBUTION TO THE EXOSPHERE TEMPERATURE OF "HOT JUPITERS"

When T_∞ is large and the thermal escape parameter X ($X = GMm/kT_\infty r$; where G is the gravitational constant, M is the planetary mass, and r is the planetocentric distance) reaches values between 3 and 1.5, the exosphere becomes unstable and hydrostatic equilibrium no longer applies (Öpik 1963). For larger values of X , the escape flux is given by the Jeans equation (Öpik 1963; Chamberlain 1963) $\phi_{\text{Jeans}} = (v_0/2\pi^{1/2})n_\infty(1+X)e^{-X}$, where n_∞ is the density of the escaping constituent at the exobase and $v_0 = (2kT_\infty/m)^{1/2}$ is the most probable velocity of exospheric particles. Note that the fraction of escaping particles becomes small (10^{-9}) if $X \approx 20$ and is negligible for values $X \geq 30$, where it drops below 10^{-13} (Bauer 1973; Watson et al. 1981).

To estimate T_{XUV_∞} for giant exoplanets, we scale Jupiter's calculated values of T_{XUV_∞} and T_0 . Using also the XUV flux evolution law in § 3, in Figure 1 we show T_{eff} and T_{XUV_∞} as a function of the orbital distance for planets around solar-type stars of different ages. T_{XUV_∞} , T_{XUV} , T_0 , g , and the I_{XUV} flux are used as scaling parameters (Smith & Hunten 1990; Gross 1972; Atreya et al. 1989). Because $T_{\text{eff}} \approx T_0$ for hydrogen-dominated planets (Smith & Hunten 1990; Atreya et al. 1989), T_{eff} can be used instead of T_0 . Values of $T_{\text{XUV}_\infty} \approx 140$ K are obtained for Jupiter-size planets at 5 AU by considering only the heating caused by stellar XUV radiation (Gross 1972). However, the dashed lines in Figure 1 show that additional heating processes are important at large orbital distances, while at distances ≤ 0.3 AU, the heat input by the present solar XUV flux alone can be sufficient to result in exospheric blow-off (*solid lines*). One can see that T_{XUV_∞} reaches values on the order of $\approx 10,000$ K as suggested by Schneider et al. (1998) and Moutou et al. (2001). Our study suggests that hydrodynamic conditions may

have occurred at distances of up to 1 AU in the past because of the young star's expected higher XUV flux. It should also be noted that our estimate may even be conservative, since neglected heating processes other than XUV irradiation may be significant also at small orbital distances.

5. ATMOSPHERIC EXPANSION AND HYDRODYNAMIC ESCAPE

For $T_\infty > 2 \times 10^4$ K ($X < 3$), the thermal energy becomes comparable to the gravitational potential energy ($3kT_\infty > 2MmG/r$), the exosphere cools down because of expansion, and the gas flows away, limited only by the incoming XUV flux (Öpik 1963; Chamberlain 1963; Watson et al. 1981). As shown in Figure 1, the closest hot Jupiters reach blow-off conditions for all the stellar ages considered. Then, the loss of particles affects the hydrostatic structure of the atmosphere and T_∞ itself, thus invalidating the application of the scaling law in equation (3) and Jeans escape. In such a case, hydrodynamic treatment must be considered (Watson et al. 1981), in which the upper atmospheric temperature, the atmospheric expansion, and the mass loss are tightly coupled. Energy-limited loss (L_{hyd}) in hydrogen-dominated atmospheres (Watson et al. 1981; Zahnle et al. 1990) can be written as

$$L_{\text{hyd}} = \frac{4\pi r_0 r_1^2 I_{\text{XUV}_\infty}}{GMm} \quad (\text{s}^{-1}). \quad (6)$$

In this relation, I_{XUV_∞} is the effective XUV heat flux averaged over the planetary sphere, r_0 is the altitude below which the gas is bound to the planet and no escape takes place, and r_1 is the altitude where the bulk of the XUV is absorbed. Because of the hydrodynamic expansion, r_0 and r_1 are usually much higher than the altitudes where the visible opacity is near unity. The altitude r_0 corresponds to an escape factor greater than 20, for which about 1×10^{-9} of the particles are escaping. (Note that Watson et al. 1981 suggested $X_0 \approx 30$ as the relevant value, for which less than 1×10^{-12} particles are escaping.) We solve simultaneously the equations for the flux of the escaping particles and the escape parameter X_1 to calculate the expansion radius r_1 (Watson et al. 1981):

$$\zeta_m = \frac{2}{s+1} \left[\frac{(X_1/2)^{(s+1)/2+1}}{X_0 - X_1} \right]^2, \quad (7)$$

where $\zeta_m = L_{\text{hyd}}(k^2 T_0 / \kappa_0 GMm)$ is a dimensionless flux parameter,

$$X_1 = \left(\frac{\beta}{\zeta_m} \left\{ X_0 - \left[\frac{2}{(1+s)\zeta_m} \right]^{1/2} \right\}^{-1} \right)^{1/2}, \quad (8)$$

where $\beta = I_{\text{XUV}_\infty}(GMm/kT_0 2\kappa_0)$ is a dimensionless energy parameter, and κ_0 is a thermal conductivity parameter of $\approx 4.45 \times 10^4$ ergs $\text{cm}^{-1} \text{s}^{-1} \text{K}^{-1}$ (Watson et al. 1981; Hanley, McCarty, & Interman 1970). The expansion radius $r_1 = (X_0/X_1)r_0$ is about 3 planetary radii (r_{pl}) if $X_0 \approx 30$ and about 4 planetary radii if $X_0 \approx 20$. By using $X_0 = 30$ (Watson et al. 1981), r_1 agrees well with the observed expanded exosphere of HD 209458b of $\approx 3r_{\text{pl}}$ (Vidal-Madjar et al. 2003).

Figure 2 shows the expansion of the atmosphere for $X_0 = 30$ and $X_0 = 20$ driven by the present solar XUV flux (*solid lines*) and by the higher flux of a 0.1 Gyr solar-type star (*dashed lines*) as function of orbital distance. As discussed before, the

increasing T_{∞} displaces the exobase to higher altitudes until the Jeans treatment is no longer valid ($X < 3$) and a hydrodynamic approach must be used (Watson et al. 1981).

6. RESULTS

By solving equations (7) and (8) for HD 209458b, we obtain an expansion radius of $r_1 = (X_0/X_1)r_0 \approx 3r_{\text{pl}}$ corresponding to a present mass-loss rate of $\approx 10^{12} \text{ g s}^{-1}$, which is in good agreement with the value measured by Vidal-Madjar et al. (2003) from planetary transit observations. Indeed, they determined a lower limit to the escape rate of $\approx 10^{10} \text{ g s}^{-1}$ that can be orders of magnitude higher because of the saturation of the absorption line (A. Vidal-Madjar 2003, private communication). For comparison, the escape rate resulting from Jeans escape at a temperature equal to T_{eff} is less than 1 g s^{-1} . For OGLE-TR-56b, currently the other exoplanet with a measured radius, we estimate a present mass-loss rate of $\approx 5 \times 10^{12} \text{ g s}^{-1}$. Our calculations, which are illustrated in Figure 3, were made with the published planetary characteristics resulting from the planetary transit analysis (Konacki et al. 2003). In this case, the mass-loss rates that we derive are even larger than former estimations of nonthermal ion escape of the order of $\approx 10^{10} \text{ g s}^{-1}$ (Guillot et al. 1996). Figure 3 shows that HD 209458b and OGLE-TR-56b may have lost by evaporation a significant fraction of their original masses during their lifetime.

In contrast with terrestrial planets, where hydrogen is a minor atmospheric constituent and is supplied by diffusion from lower

altitudes, hydrogen-dominated giant planets do not have a source from below until they shrink to their core sizes or heavier constituents become dominant. A detailed study addressing diffusion-limited atmospheric escape is beyond the scope of this work, but a study is in progress, in which we will consider a multicomponent composition of light and heavy constituents.

Giant gaseous exoplanets with small initial masses may evolve into volatile-rich large terrestrial planets (Kuchner 2003; Lammer et al. 2003b). This process could explain the observed paucity of massive close-in exoplanets (Pätzold & Rauer 2002). The remnant cores of giant exoplanets orbiting close to their host stars may be detectable for the first time with the new generation of space observatories such as *Convection and Rotation (COROT)* or *Kepler*. In conclusion, our study shows that thermal escape at close orbital distance, once claimed to be negligible, is a major loss process that should be included in any realistic model of the mass and radius evolution of close-in exoplanets.

H. Lammer, I. Ribas, and F. Selsis thank the Österreichischer Akademischer Austauschdienst (ÖAD) for supporting this work, which is part of the Austrian-Spanish program Acciones Integradas, project 7/2001 related to the evolution of planetary paleo-atmospheres. W. W. Weiss thanks the Austrian Ministry for Science, Education and Culture (bm:bwk) for supporting the *COROT* project. E. F. Guinan and I. Ribas acknowledge support from NASA/*FUSE* grants NAG5-10387 and NAG5-12125.

REFERENCES

- Atreya, S. K., Pollack, J. B., & Matthews, M. S. 1989, *Origin and Evolution of Planetary and Satellite Atmospheres* (Tucson: Univ. Arizona Press)
- Ayres, T. R. 1997, *J. Geophys. Res.*, 102, 1641
- Bauer, S. J. 1971, *Nature*, 232, 101
- . 1973, *Physics of Planetary Ionospheres* (Heidelberg: Springer)
- Bauer, S. J., & Hantsch, M. H. 1989, *Geophys. Res. Lett.*, 16, 373
- Chamberlain, J. W. 1963, *Planet. Space Sci.*, 11, 901
- Cho, J. Y.-K., Menou, K., Hansen, B. M. S., & Seager, S. 2003, *ApJ*, 587, L117
- Cody, A. M., & Sasselov, D. D. 2002, *ApJ*, 569, 451
- Del Popolo, A., & Eksi, K. Y. 2000, *MNRAS*, 332, 485
- Gross, S. H. 1972, *J. Atmos. Sci.*, 29, 214
- . 1974, *J. Atmos. Sci.*, 31, 1413
- Guillot, T., Burrows, A., Hubbard, W. B., Lunine, J. I., & Saumon, D. 1996, *ApJ*, 459, L35
- Guinan, E. F., & Ribas, I. 2002, in *ASP Conf. Ser. 269, The Evolving Sun and Its Influence on Planetary Environments*, ed. B. Montesinos, A. Gimenez, & E. F. Guinan (San Francisco: ASP), 85
- Hanley, H. J. M., McCarty, R. D., & Interman, H. 1970, *J. Res. NBS*, 74, 331
- Hubbard, W. B., Burrows, A., & Lunine, J. I. 2002, *ARA&A*, 40, 103
- Johnson, R. E. 1990, *Energetic Charged-Particle Interactions with Atmospheres and Surfaces* (Heidelberg: Springer)
- Konacki, M., Torres, G., Jha, S., & Sasselov, D. D. 2003, *Nature*, 421, 507
- Kuchner, M. J. 2003, *ApJ*, in press
- Lammer, H., Lichtenegger, H. I. M., Kolb, C., Ribas, I., & Bauer, S. J. 2003a, *Icarus*, 165, 9
- Lammer, H., Selsis, F., Ribas, I., Lichtenegger, H. I. M., Penz, T., Guinan, E. F., Bauer, S. J., & Weiss, W. W. 2003b, in *Towards Other Earths (Darwin/TPF)*, ed. B. Battrick (ESA SP-539; Noordwijk: ESA), in press
- Moutou, C., Coustenis, A., Schneider, J., St. Gilles, R., Mayor, M., Queloz, D., & Kaufer, A. 2001, *A&A*, 371, 260
- Öpik, E. J. 1963, *Geophys. J. RAS*, 7, 490
- Pätzold, M., & Rauer, H. 2002, *ApJ*, 568, L117
- Sasselov, D. D. 2003, *ApJ*, 596, 1327
- Schneider, J., Rauer, H., Lasota, J. P., Bonazzola, S., & Chassefière, E. 1998, in *ASP Conf. Ser. 134, Brown Dwarfs and Extrasolar Planets*, ed. R. Rebolo, E. L. Martin, & M. R. Zapatero Osorio (San Francisco: ASP), 241
- Simon, T., Boesgaard, A. M., & Herbig, G. 1985, *ApJ*, 293, 551
- Smith, G. R., & Hunten, D. M. 1990, *Rev. Geophys.*, 28, 117
- Stallard, T., Miller, S., Millward, G., & Joseph, R. D. 2002, *Icarus*, 156, 498
- Vidal-Madjar, A., Lecavalier des Etangs, A., Désert, J.-M., Ballester, G. E., Ferlet, R., Hébrand, G., & Mayor, M. 2003, *Nature*, 422, 143
- Watson, A. J., Donahue, T. M., & Walker, J. C. G. 1981, *Icarus*, 48, 150
- Wuchterl, G., Guillot, T., & Lissauer, J. J. 2000, in *Protostars and Planets IV*, ed. V. Mannings, A. P. Boss, & S. S. Russell (Tucson: Univ. Arizona Press), 1081
- Zahnle, K., Pollack, J. B., & Kasting, J. F. 1990, *Icarus*, 84, 503
- Zahnle, K. J., & Walker, J. C. G. 1982, *Rev. Geophys. Space Phys.*, 20, 280